Proceeding of ICFDP7
Seventh International Conference of Fluid Dynamics and Propulsion
December 18-20, 2001, Cairo, Egypt

ICFDP7-2001076

A Computational Investigation of the Back Step Flow

Atef O. Sherif
Department of Aerospace
Faculty of Engineering, Cairo University
Giza 12613 - Egypt

Mohamed A. Hussein
Flow Visualization Lab. Department of Aerospace
Faculty of Engineering, Cairo University
Giza 12613 - Egypt

Abstract

This paper reports on a current work in the flow visualization Lab. to study the internal backward facing flow. The problem is well known, very relevant from engineering point of view, and exhibits complicated flow phenomena; laminar separated flow, multiple re-circulating flow regions and vortex shedding that may lead to self-excited oscillations. An interactive solver for laminar two-dimensional incompressible flow was developed using vorticity-stream function formulation. The solver is equipped with an automatic detector of separation/ reattachment zones and a load prediction tool. To validate the versatility of the solver a standard test problem for backward facing flow. Computed results are compared to other published computational and experimental results. Streamlines, Vorticity and pressure patterns are reported in addition to histories of forces generated on the problem configuration and trajectories of loading center. Computational time requirements on PC configurations are addressed. The developed solver is extendible to turbulent, compressible and three-dimensional flows.

1. Introduction

The Backward Facing Step is a famous classical problems that received, and is still receiving, wide interest in literature. The problem is very relevant from engineering point of view, exhibits multiple recirculating flow regions and vortex shedding and is considered as a tough benchmark and a severe test for computational mehods.

Theroetical investigations to understand the structure of the flow and investigate the properties of the base flow at very low reynolds numbers are given in [1]. Extensive experimental results using laser Doppler measurements which first identified the three recirculating flow zones characterizing the laminar flow at relatively high Reynolds numbers are reported in [2]. The work also surveys all relevent experimental works at the time and includes a computation of the problem.

Several computational works are reported in literature. Usually primitive variables formulation of the two-dimensional incompressible Navier Stokes equations is used with either of the two approaches artificial compressibility and the pressure Poissons equation.

Chorin [3], modified the continuity equation by adding a time derivative for the pressure. Thus, the flow becomes artificially compressible. The approach suffers the introduction of pressure waves of finite speed in the flow field. The governing equations are hyperbolic requiring methods developed for compressible flow. Explicit fourth order dissipation terms were added to the continuity equation to prevent the odd-even decoupling modes in the pressure field. The approach is generally used when steady solutions are sought.

Harlow and Welch [4], replaced the continuity constraint by a Poisson equation for the pressure. The governing equations consisted of parabolic momentum equations and the elliptic pressure Poisson's equation. Boundary conditions were required for the pressure. To satisfy the continuity equation they proposed to used staggered grid to prevent grid scale oscillations.

Sotiropoulos and Abdallah [5], carefully examined the problem that Poisson's based methods may not satisfy the discrete continuity equation exactly on a non-staggered grid. Further works indicated that integrability and regularity were two important constraints that should be considered in the discretization process.

Forin etal [6], applying to a test backward facing step, addresed the question of stability of numerical solutions of the incompressible Navier-Stokes equations in the linear

hydrodynamic sense? Their work was an answer to the controversy conserning stability of such flow claimed by Kaiktsis etal [7]. They detrmined the range of stability of the problem. Similar arguments were raised by Gercho etal [8].

Differences in reported efforts were categorized into two main domains: improving and obtaining better schemes; and the treatment of the boundary and initial conditions. The treatment of the boundary conditions vitally affected the quality of the obtained solution, solution's response and the time to reach the steady state.

This work is a first in a series to revisit the backstep flow problem in the light of the new developments of power and capacity of personal computers. The problem considered is that of internal laminar two-dimensional flow past a backstep at relatively low Reynold's numbers, O (10^2-10^3) using the vorticity-stream function equations. The target is to study the properites of the flow problem and the productivity and effectiveness of utlizing personal computers in this area. This is specially relevant in developing countries which are usually short of advanced computational facilities. For this an interactive flow solver is developed as an extesion to work presented in [9].

2. Nomenclature

List of Symbols

c	Local coefficient of friction.
C	Coefficient of friction.
a_x, a_y	Diffusion coefficient.
Re	Reynolds number. Also, residual of computations.
Q	Smoothing factor.
S	Boundary of a domain.
t	Time.
u, v	Velocity component along coordinates.
$\underline{U}$, $\underline{V}$	Velocity vector.
x, y	Distance along Cartesian coordinates.
$\underline{x}$	Position vector.

Greek Symbols

Δ	Increment of time or space.
Ψ	Stream-function.
ζ	Vorticity.
ω	SOR factor.

Latin Subscripts

i	Index of nodes along X_1-axis.
j	Index of nodes along X_2-axis.
m	Mean.
k	Iteration number
n	Time step number

3. Problem formulation

The Back Step Problem.

Consider the two-dimensional internal bounded flow of an incompressible viscous fluid past a finite back step as shown in fig.1. The geometry and the boundary conditions of the test problem were defined in the second mini symposium on open boundary conditions by Sani and Gresho [10]. The geometry is charactrized by the inlet expansion ratio (Step height/chanel height =½) and the length to height ratio (Length/height =20). The flow reynolds number is based on the mean inlet velocity and the chanel height. The inlet velocity distribution for the laminar case is assumed fully developed parabolic.

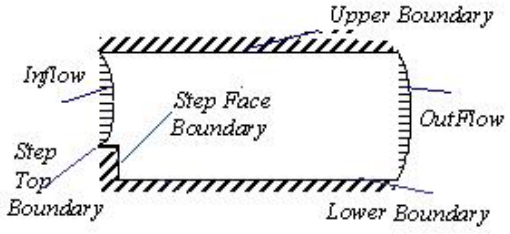

Fig.1 *Sketch of the problem, the step is enlarged here for explanatory reasons only.*

The Governing Equations

The vorticity-stream function formulation describing the unsteady, compressible, three-dimensional Navier-Stokes equations can be written in vector form in terms of a three-dimensional vector potential, Ψ, and vorticity vectors, [11]. The mass flux is then defined as the curl of the vector

potential, $\rho\vec{V} = Curl\ \vec{\Psi}$, while the vorticity is defined as the curl of velocity, $\vec{\zeta} = Curl\,\vec{U}$.

For unsteady 2-D incompressible flows only one component of the generalized potential need be considered. Neglecting external gravity forces the governing equations are: -

$$\nabla^2\psi = -\zeta \qquad (1)$$

$$\frac{\partial\zeta}{\partial t} + (\vec{U}.\vec{\nabla})\zeta = R_e^{-1}\nabla^2\zeta \qquad (2)$$

where ψ is the two dimensional stream function, ζ the vorticity, t denotes time and R_e is the flow Reynolds number.

The energy equation is decoupled and is evaluated after a *solution* has been found. The pressure distribution is obtained by solving:

$$\frac{1}{\rho}\nabla^2 p = -\vec{\nabla}.\left(\vec{V}.\vec{\nabla}\right)\vec{V} \qquad (3)$$

where p is the static pressure and ρ is the flow density;

Where: $\vec{U} = \begin{bmatrix} \frac{\partial}{\partial y}\psi \\ -\frac{\partial}{\partial x}\psi \end{bmatrix}$ (4)

Subject to proper initial and boundary conditions for the stream function, the vorticity and the pressure.

4. Problem Discretization and Algorithm

Discritization of the domain.

The domain, is discritized using stretched cartesian grid with considerable concentrations at the locations where separation reattachment are likely to occur and at locations where high gradients are expected , figure 2.

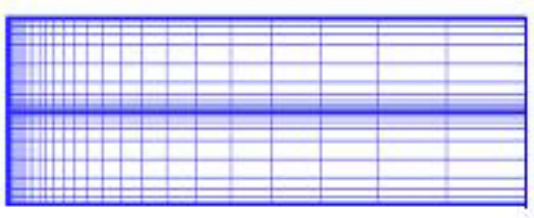

Figure.2 *Discretized Physical domain of the problem*

The stretching/concentration of the grid was constrained by an arbitrary user selectable minimum of the spatial steps

Discretization of the Stream–Function equation.

A five point centered difference approximation was used . The recurrence relation used for the stretched grid is:

$$\psi_{ij}^{t+1} = \frac{\left[a_x\left[\psi_{i+1,j}^t + f_x\psi_{i-1,j}^t\right] + a_y\left[\psi_{ij+1}^t + f_y\psi_{ij-1}^t\right] + \zeta_{ij}^t\right]}{a_x(1+f_x) + a_y(1+f_y)} \qquad (5)$$

Where:

$$a_x = \frac{2fx}{(1+f_x)\Delta x_i^2} \quad and \quad a_y = \frac{2f_y}{(1+f_y)\Delta y_j^2} \qquad (6)$$

and

f_x and f_y are the local cell stretching in the x- and y-directions.

Discretization of the Vorticity–Transport Equation.

Diffusion terms were discretized using a five point centered difference approximation. Convection term were discretized using a first order upwind scheme and a forward differencing for the time derivative. The recurrence relation used is:

$$\zeta_{ij}^{t+1} = \zeta_{ij}^{t} - C_X - C_Y + \frac{dt}{\mathrm{Re}}\left(D_X + D_Y\right) \qquad (7)$$

Where :

C_X and C_Y are convected Vorticity in x & y directions.
D_X and D_Y is the diffused Vorticity in x- and directions.

$$C_X = \frac{dt}{dx}Uc\,D\zeta_x \quad and \quad C_Y = \frac{dt}{dx}Vc\,D\zeta_y \qquad (8)$$

where;

$$\begin{aligned} U_c &= (U_{i-1,j}+U_{i,j})/2 \quad for\ U_{i,j} > 0 \\ &= (U_{I+1},j+U_{i,j})/2 \qquad U_{i,j} < 0 \\ V_c &= (V_{i,j-1}+V_{i,j})/2 \quad for \quad V_{i,j} > 0 \\ &= (V_{i,j+1}+V_{i,j})/2 \qquad V_{i,j} < 0 \end{aligned} \qquad (9)$$

$$\begin{aligned} D\zeta_x &= (\zeta_{ij} - \zeta_{i-1,j}) \quad for \quad U_{i,j} > 0 \\ &= (\zeta_{i+1,j} - \zeta_{ij}) \qquad U_{i,j} < 0 \\ D\zeta_y &= (\zeta_{ij} - \zeta_{i,j-1}) \quad for \quad V_{i,j} > 0 \\ &= (\zeta_{I+1\,j} - \zeta_{i,j}) \qquad V_{i,j} < \end{aligned} \qquad (10)$$

The second derivatives D_x and D_y of the Vorticity and were approximated using;

$$D_X = \frac{2\,fx\,(\zeta_{i+1,j} + fx\,\zeta_{i-1,j} - (1+fx)\zeta t_{i,j})}{\Delta x_i^2\ fx+1} \qquad (11)$$

$$D_Y = \frac{2\,fy\,(\zeta_{i,j+1} + fy\,\zeta_{i,j-1} - (1+fy)\zeta_{i,j})}{\Delta y_j^2\ fx+1} \qquad (12)$$

The resulting algebraic equations for both the stream function and the vorticity were solved using point successive over relaxation method.

Discretization of the boundary conditions.

Sani and Grecho [10] defined the boundary conditions for the test problem as; parabolic inlet velocity profile, no slip boundary condition on the solid walls and pressure related outflow condition.

Gresho and Sani [12], gave an extensive review of the proper boundary conditions. No slip condition with solid boundaries, homogeneous and non-homogeneous Neumann boundary conditions for the pressure, Dirichlet type boundary condition for the pressure at the outflow boundary and Neumann condition for the tangential velocity component.

The Inflow condition is evaluated for the stream function by numerically integrating the given discretized parabolic inflow profile. The boundary condition for the vorticity is obtained by numerically differentiating the same velocity profile using centered differencing for the regular grid points and one-sided differencing at the solid walls.

On the lower boundary, the stream function is constant (zero). To ensure the satisfaction of the no slip condition, the near solid boundary points are forced to lie on a linear velocity profile between the solid boundary and the next interior point.

$$\psi_1 = \psi_0 + \frac{1}{(1+f_y)^2}(\psi_2 - \psi_0) \qquad (13)$$

The vorticity is extrapolated from the interior grid points using 3 point one-sided differencing.

$$\zeta_{i,0} = \frac{2\,(\psi_{i,2} - (1+fy)\psi_{i,1} + fy\,\psi_{i,0})}{\Delta y_0\, fy(1+fy)} \qquad (14)$$

The upper solid boundary is treated similarly with constant value for the stream function (1) and the near boundary treatment is similar to the lower boundary, equation (13). A three point one-sided differencing extrapolation for the vorticity is used similar to equation (14).

The outflow boundary is treated similar to the inflow for the stream function values. The vorticity is the convected out using one sided differencing.

$$\zeta_{i\max,j} = \zeta_{i\max-1,j} \qquad (15)$$

The back step face is part of the lower solid boundary and is treated the same for the stream function including the near boundary treatment, equation (13). For the vorticity, an expression similar to equation (14) is used.

In addition, an initial divergence free velocity field is required to start the solution. As indicated by LE et al [13], a predictor needed is used to generate smooth velocity distribution. Here, the stream function equation is solved and then the velocity field is evaluated.

The Solution Algorithm:

The following algorithm is used to construct the program:

1. Define Re, Δx_{min}, IMax, JMax and maximum run time.
2. Estimate Δy_{min}, and Δt, ω
3. Construct appropriate grid.
4. Apply ψ boundary conditions.
5. Construct initial solution for ψ.
6. Construct velocity field
7. Construct initial solution for the vorticity.
8. Apply ζ boundary conditions.
9. Advance time.
10. Estimate new internal solution for ψ
11. Smooth the stream function solution using
$$\psi_{i,j}^{n} = \psi_{i,j}^{n} Q_1 + (1-Q_1)\psi_{i,j}^{n-1} \qquad (16)$$
12. Calculate the new Velocity field
13. Advance the Vorticity in time.
14. Smooth the vorticity distribution using.
$$\zeta_{i,j}^{n+1} = \zeta_{i,j}^{n} Q_1 + (1-Q_1)\zeta_{i,j}^{n+1} \qquad (17)$$
15. Save the new computed values
16. Repeat from step 8 until the stream function and vorticity values converge or maximum time exceeded.
17. Compute the pressure distribution
18. Detect separations/reattachments and compute integral properties; skin friction, forces and line of action of force, etc.
19. End algorithm

The convergence Criteria

The convergence criteria used in this work is based on convergence of the maximum residual in the field for both the stream function and the vorticity:

Functional evaluation

Velocity profiles are calculated using centered differencing at all reular internal points. Pressure was evaluated by solving the pressure Poissons equation. The coefficient of friction is calculated from the computed vorticity distribution: as

$$c_{f_i} = 2\frac{\zeta_{i,0}}{R_x} \quad (18)$$

Integral description of forces is obtained by direct integration of pressure and friction

$$C_F = \int_{X_{LE}}^{X_{TE}} c_f(x)\,dx \quad (19)$$

$$c_n = \frac{1}{c}\left[\int_0^c (C_{p,l} - C_{p,u})dx + \int_{LE}^{TE} (c_{f,u} + c_{f,l})dy\right] \quad (20)$$

$$c_a = \frac{1}{c}\left[\int_{LE}^{TE} (C_{p,u} - C_{p,l})\,dy + \int_0^c (c_{f,u} + c_{f,l})dx\right] \quad (21)$$

$$c_{mle} = \frac{1}{c^2}[\int_0^c (C_{p,u} - C_{p,l})xdx - \int_{LE}^{TE} (c_{f,u} + c_{f,l})xdy + \int_{LE}^{TE} (C_{p,u} - C_{p,l})ydy + \int_0^c (c_{f,u} + c_{f,l})ydx] \quad (22)$$

$$C_L = c_n \cos\alpha - c_a \sin\alpha$$
$$C_D = c_n \sin\alpha + c_a \cos\alpha \quad (23)$$

where

C_p, C_f, C_n and C_a are the local pressure, friction, normal and axial force coefficients, respectively.

C_L, C_D and C_m are the lift, drag and pitching moment coefficients, respectively. Forces are obtained by multiplying coefficients by $\frac{1}{2}\rho V^2 * Area$.

u and *l* are subscripts referring to upper and lower surfaces, respectively.

5. Results and Discussion

The interactive program was developed using Microsoft Visual Basic for the interface. To optimize, the program performance, C++ DLLs were developed and called to perform the computing intensive modules.

Several case studies were performed using several grids: 128*32 and 128*64 and 256*64 to make sure solution is grid independent. Each study was given enough time steps to reach steady state, and all the results were compared with experimental results [2]

Case Study 1: Dependence of the locations of separation/reattachment on time and their steady state values

In this case the Reynolds Number is held constant at 400 while varying the number of time steps in order to reach the steady state solution. Figure.3 explains the notation used for separation and reattachments. X1, X2 and X3 are plotted versus time steps.

Using a 128 x 64 grid (8,192 grid points), it is Clear from, Figure.4 that the main re-circulation zone, X1, is preserved all over to the steady state.

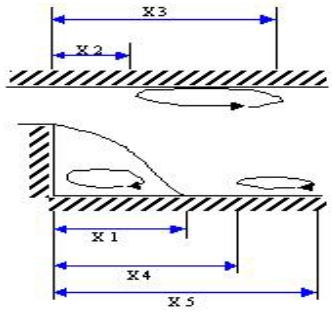

Figure.3 *Notation for the Location Separation and Reattachment*

The upper, X2, and the second lower, X4, circulation zones vanish after about 16,000 time steps. X1 almost reached a steady state at about 100,000 time steps.

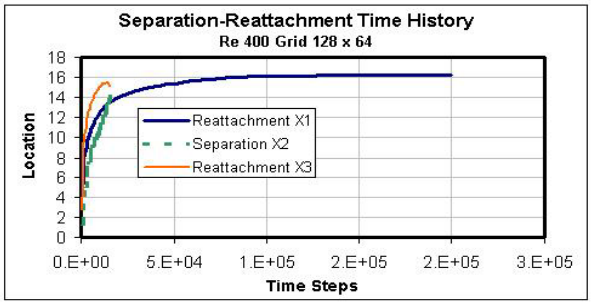

Figure.4 Separation and Reattachment Locations Vs Time Steps for a grid 128 x 64 and Re=400

The run time was about 50 seconds for this case using Pentium IV-1.7 GHz. Note that, Ref. [2] used TEACH code, a 45 x 45 grid (2025 grid points) and 1200 iterations on a UNIVAC-1108. The run time was 75 minutes. It was not possible at the time to run grid point counts over 2600.

Figure 5 shows similar computation using a 256x 128 grid; the steady state solution was reached after about 85,000 time steps for the three re-circulating zones.

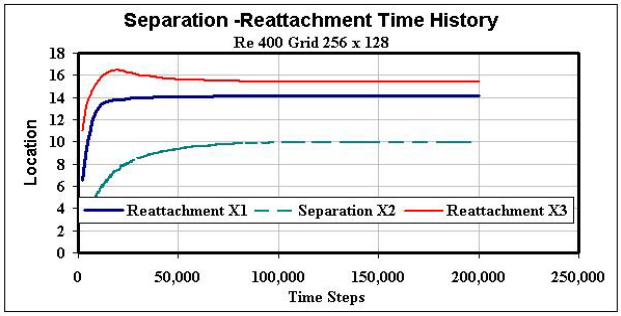

Figure.5 Separation and Reattachment Locations Vs Time Steps for a grid 256 x 128

There is a slight change in the reattachment point X3 at 150,000 but this is acceptable within the current working precision. Thus, increasing the grid resolution helped to speed up convergence to steady state as well as capturing the details of the solution. Note that earlier computations did not go far enough for the grid to dissolve the secondary structures.

Case Study 2: Effect of the Reynolds Number on the Locations of Separation and Reattachment

In this study the Reynolds number was raised from 400 to 1200 with a step 50 for 100,000 time steps under the laminar flow assumption following Ref [2] experiments.

Defining X1, X2 and, X3, as Shown in the figure.3, figure.6 shows how the results varied with the Reynolds number as compared to the experimental results.

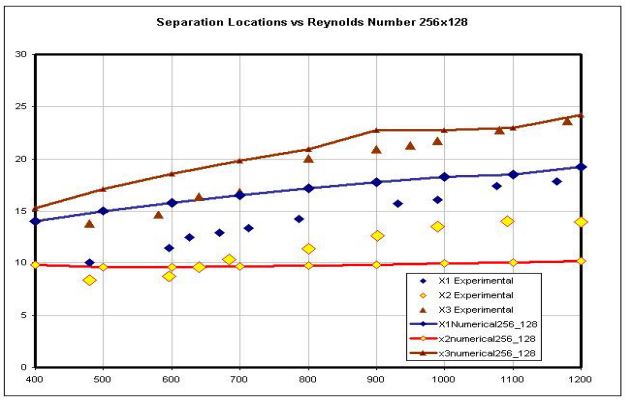

Figure.6 Locations of Separation / Reattachment Vs Reynolds Number at T=50 Sec. (100,000 Time Steps) compared to the experiment [2]

For the 128*48 Grid, the numerical results for X1 and the experiment seem to be taking the same trend with reasonable agreement with experiment.

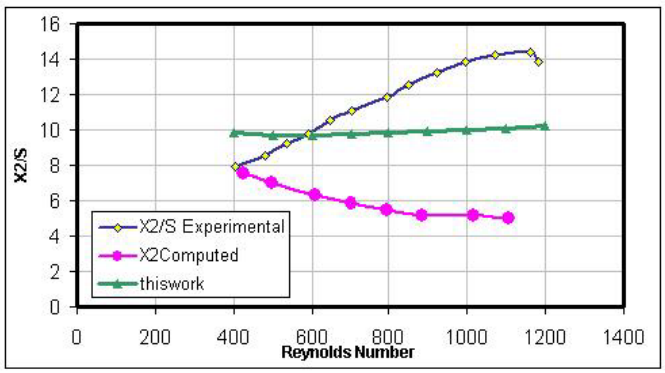

Figure.7 Locations of Separation, X2, on upper surface Vs Reynolds Number at T=50 Sec. (100,000 Time Steps) compared to experiment and computation of [2].

Figures 7 and 8 compare the current computation to both the experimental and computational work of Ref. [2]. There seems a problem with X2, which for this grid resolution doesn't follow the experimental trend as close as X1 & X3.

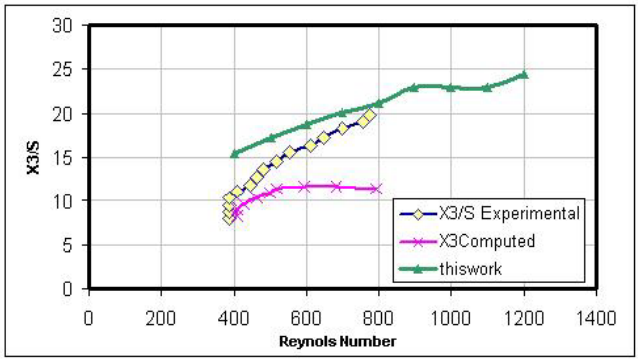

Figure.8 Locations of secondary Separation, X3, on lower surface vs. Reynolds Number at T=50 Sec. (100,000 Time Steps) compared to experiment and computation of [2]

In figure.9 and figure.10 the present results are compared with numerical and experimantal results of [2]. Contradiction between his numerical and experimental work are obvious. The current computations clearly demonstrated better agreement with experiment for X3 and are much closer to the experiment especially at higher Reynolds number.

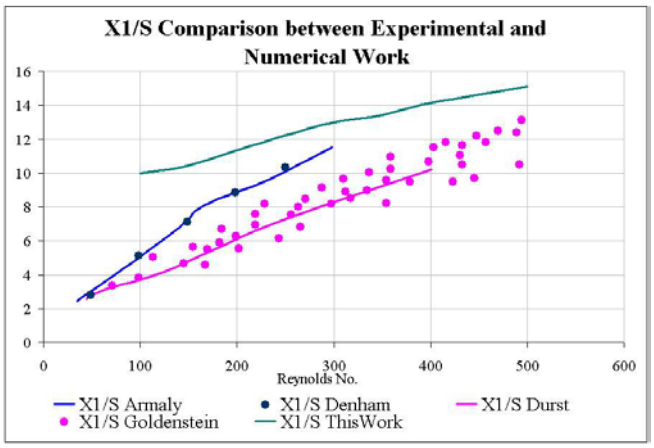

Figure 9. X1/S comparison between Experimental, Numerical of [2] [14] , [15] , [16]

The above figure.9 shows a comparison between this works and [2] [14-16], with a general good agreement. This supports the conclusion that the current solver is both reliable and satisfactory.

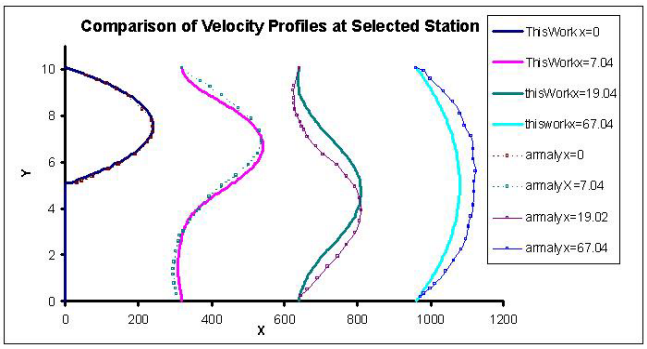

Figure 10. Velocity Distributions at selected station, comparison with Experimental Ref. [2].

Figure.10 shows comparison between computed velocity profiles and measurements of Ref. [2]. The comparison is excellent at the early stations. Discrepancies at later stages may be attributed to deviations from parabolic input and output profiles that Ref. [2] reported.

Case Study 3: Flow Structure, Pressure contours, Total force and Location of center of pressure

The following sequence of shots in Figure.11 demonstrates the effect of Reynolds number on the transient development of the solution. Secondary, ternary and higher resolution vortices temporarily appear complicating the flow structure. In the last two frames five vortices are spotted.

Figure 12 and 13 show pressure contours for Reynolds numbers 400 and 1200. With clear greater expansion and stronger pressure at the higher Reynolds number.

Figures 14 and 15 demonstrate the locus of the resultant force acting on the channel relative to the step for the two Reynolds numbers 400 and 1200. A unit vector indicates the direction of force at the point in time. The location of resultant force changes with time during the transient solution, demonstrating a clear unsteady problem.

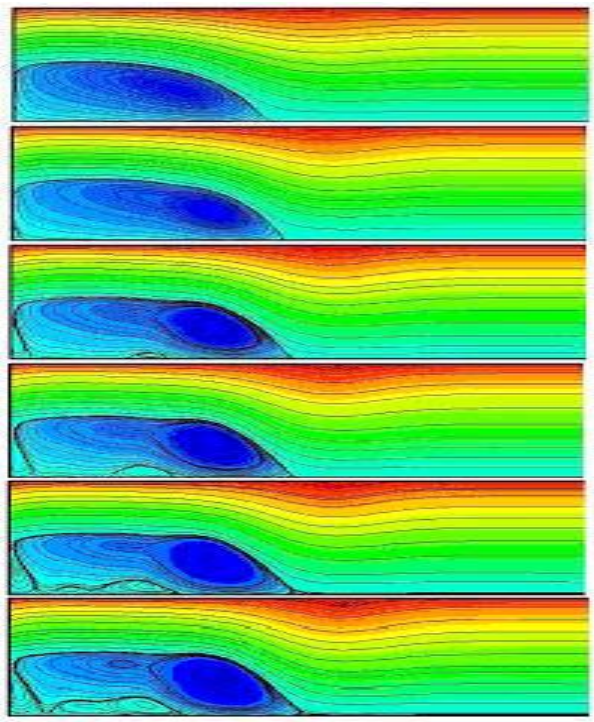

Figure.11 *Streamlines at different Reynolds Number, Grid 128 x 64.*

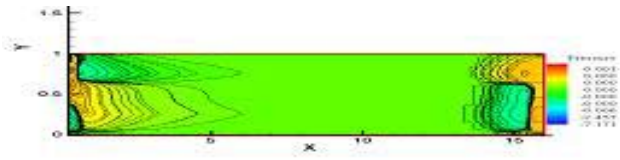

Figure.12 *Pressure Isobars for Re=400 , Grid 256 x 128*

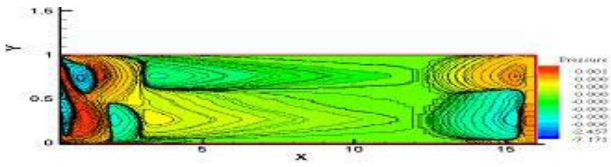

Figure.13 *Pressure Isobars for Re=1200 , Grid 256 x 128*

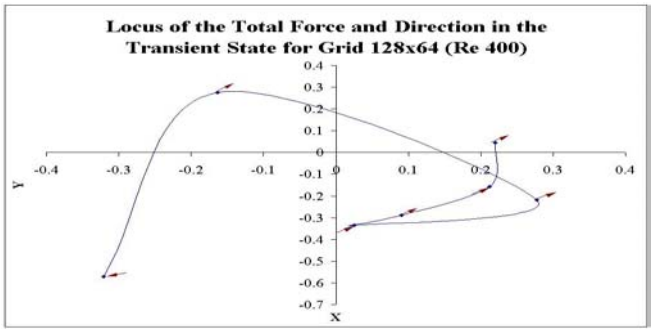

Figure.14 *Resultant force locus for different time steps at Re=400 , Grid 128.x 64*

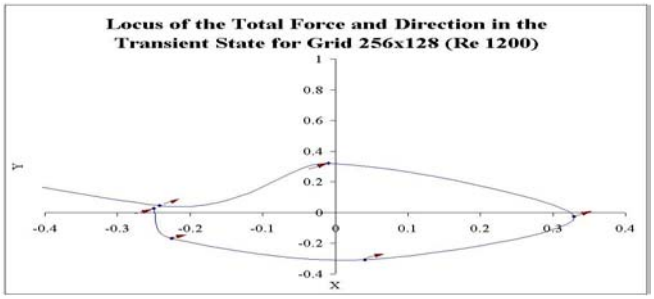

Figure.15 *Resultant force locus for different time steps at Re=1200, Grid 256 x 128*

Designers should take that in considerations while designing parts subjected to such unsteady phenomena.

6. Conclusion

- An interactive fast, reliable, flexible program has been developed and tested for the back step flow problem based on the stream function vorticity formulation.
- The treatment of boundary condition was successful; producing results that captured problem complex flow structural details with good agreement with published computational and experimental works. Separation and Reattachment locations seemed to acceptably agree with results of [2], [12-15].
- Relatively dense grids and extended time steps are required to ensure that the solution is grid independent. A reasonable choice for this approach is stretched grid with 256 x 128 node along (total of 32768 nodes) and 100,000 time steps. The Corresponding run time using current personal computers is less than one minute for such problems.
- The built in load estimation capability produced results essential for designers to consider while designing parts subjected to similar unsteady flow regimes and extremely difficult to determine experimentally.

References

1. Viviand, H. and Berger, S. A., "The base flow and near wake problem at very low Reynolds numbers: Part 1: The Stokes approximation", J. fluid mechanics, vol. 23 part 3, 417-438, 1965.
2. Armaly B.F, and Durst, F., "Experimental and theoretical investigation of backward–facing Step" Flow. Universität Karlsruhe, 1982.
3. Chorin, J. A., 'A Numerical Method for Solving Incompressible Viscous Flow Problems', J. Comp. . Phys., 212-26, 1967
4. Harlow, F. H. and Welsh, J. E., "Numerical calculation of time dependent viscous incompressible flow of fluid with free surface", Phys. Fluids., 8, 2181-2189, 1965.
5. Sotiropoulos, F. and Abdallah, S., "The discrete continuity equation in primitive variable solutions of incompressible flows", J. comp. phys., 95, 212-227, 1991.
6. Fortin, A., Jardak, M. and Gervals, J. J., Localization of Hopf bifurcations in fluid flow problems, Int., J. numer. methods fluids, 24, 1185-1210,, 1997.
7. Kaiktsis, L., Karniadakis, G. E. and Orszag, S., "Onset of three dimensionality, equilibria and early transition in the flow over a backward facing step", J. fluid mech., 231, 501-528, 1991.
8. Grecho, P. M., Gartling, D. K., Torczynski, J. R., Cliffe, K. A., Winters, K. H., Garatt, T. J., Spence, A. and Goodrich, J. W., " Is the steady viscous incompressible two dimensional flow over a backward facing step at Re=800 stable?" Int., J. numer. methods fluids, 17, 501-541,, 1993
9. Sherif, A. O., and Rashed, M. I., "Computational Simulation of the boundary layer concept", Proc. 14th Int. conf. statistics, computer science, OR and mathematics, Vol. 3., 174-190, Cairo, 1979.
10. Sani, R. L. and Gresho, P. M., " Resume and remarks on the open boundary condition mini symposium", Int, J. numer. Methods fluids, 18, 983-1008,, 1994
11. Sherif, A. O., "Vector Potential Calculations of Steady Three Dimensional Transonic Flows", The Fifth International Conference for Mechanical Power Engineering, Ain Shams University, Cairo, pp. 24-1-24-20, 1984.
12. Gresho, P. M. and Sani, R. L., "On the pressure boundary condition for incompressible Navier-Stokes equations", Int., J. numer. methods fluids, 7, 1111-1145, 1987.
13. Le, T. H., Troff, B., Sagaut, P. and Tran, K. D., "PEGASE: A Navier-Stokes solver for Direct Numerical Simulation of Incompressible Flows", Int., J. numer. Methods fluids, 24, 833-861, 1997
14. Denham, M. K & Patrick, M. A, "Laminar flow over a downstream–facing step in a two-dimensional flow channel", Trans. Inst. Chem. Engrs. 52,361,1974.
15. Goldenstein, R. J., Eriksen, V. L., "Laminar separation reattachment and transition of flow over a downstream-Facing Step. Trans. A.S.M.E.D; J. Basic Engineering, 1970
16. Durst, F. and. Pereira, J. C. F, Time dependent laminar backward facing step flow in a two-dimensional duct", 1977.

